Supporting Information

Regulating Signal Enhancement with Coordination-Coupled Deprotonation of a Hydrazone Switch

*Justin T. Foy, Debdas Ray, Ivan Aprahamian**

Department of Chemistry, Dartmouth College, 6128 Burke Laboratory, Hanover, NH 03755 (USA)

ivan.aprahamian@dartmouth.edu

Table of contents **pages**

1.1 General Methods. All reagents and starting materials were purchased from TCI-America and used without further purification. Column chromatography was performed on silica gel (Silicycle, 230-400 mesh). Silicycle glass backed thin layer chromatography (TLC) plates (extra hard layer, 60 Å, F–254 indicator) were used for all TLCs. Deuterated solvents were purchased from Cambridge Isotope Laboratories and used as received. NMR spectra were recorded on a 500 MHz spectrometer, with working frequencies of 499.8, 125.7 and 282.2 MHz for the ^{1}H, ^{13}C and ^{19}F nuclei, respectively. Chemical shifts are quoted in ppm relative to tetramethylsilane, using the residual solvent peak as a reference standard. Hi-Res mass spectra were measured on a Micromass Q-Tof Ultima at the University of Illinois, Urbana-Champaign. UV-Vis spectra were recorded on a Shimadzu UV/Vis spectrophotometer (UV-1800). Fluorescence spectra were recorded on a JASCO FP-8200 fluorometer. All spectroscopy samples were taken at room temperature. Compound **1(*E*)** was synthesized using a previously reported procedure.[S1]

1.2 Spectroscopic Methods. Absorption and fluorescence spectra were recorded using freshly prepared stock solutions in spectroscopic grade CH_3CN (Alfa Aesar). For the fluorescence measurements, the excitation/emission bandwidth was set to 5 nm and the excitation wavelength was set equal to the λ_{max} of the corresponding absorption spectrum (λ_{ex} **MBD** = 496 nm; λ_{ex} **ANI** = 405 nm). The response time was set to 1s and the sensitivity was set to low for samples with **MBD** and medium for samples with **ANI**.

1.3 Catalysis ON/OFF NMR Experiment. 10 μL of a $Zn(ClO_4)_2$ (0.2062 mg, 6.13×10^{-4} mmol) solution (0.0613 M, CD_3CN) was added to a solution of **ANI** (1 mg, 3.07×10^{-3} mmol) and **1(*E*)** (0.189 mg, 6.13×10^{-4} mmol) in CD_3CN (600 μL) and the reaction was monitored

using ^{1}H NMR spectroscopy. After 7 min, 10 μL of a (nBu$_4$)NCN solution (0.307 M, CD_3CN) was added to the mixture, and the outcome was monitored using ^{1}H NMR spectroscopy for 10 min. Afterwards, 60 μL of $Zn(ClO_4)_2$ solution was added to the mixture, and the reaction was monitored until its completion using ^{1}H NMR spectroscopy.

2. Synthesis

1,3,5,7-tetramethyl-8-(4-morpholinophenyl)-4,4-difluoro-4-bora-3a,4a-diaza-s-indacene MBD). This compound was synthesized using a modified literature procedure.[S2] 2,4-Dimethylpyrrole (1.1 mL, 2 equiv, 10.48 mmol) was added to a solution of (*p*-formylphenyl)morpholine (1.00 g, 1 equiv, 5.24 mmol) dissolved in dry dichloromethane (200 mL), followed by a drop of TFA. After stirring overnight, a solution of 2,3-dichloro-5,6-dicyanobenzoquinone (1.00 g, 1.2 equiv, 6.28 mmol, 10 mL dry dichloromethane) was added dropwise. The mixture was allowed to stir for 1 h upon which diisopropylethylamine (6.51 mL, 7.1 equiv, 37.4 mmol) and boron trifluoride etherate (8.38 mL, 5.3 equiv, 27.0 mmol) were added. The reaction mixture was then allowed to stir for an additional two hours before being concentrated *in vacuo.* The crude residue was redissolved in dichloromethane (50 mL) and filtered through a celite plug. The organic layer was washed with water (3 × 100 mL) before a final wash with brine. The organic layer was dried over anhydrous sodium sulfate and concentrated *in vacuo*. Column chromatography was used to purify the crude residue (SiO_2, hexanes/ethyl acetate/triethylamine, 7:3:0.01, R_f = 0.15) to yield 399 mg (19% yield) of the pure compound as an orange powder. m.p. 268 ± 1 °C. ^{1}H NMR (500 MHz, CD_2Cl_2) δ 7.15 (d, J = 8.79 Hz, 2H), 7.01 (d, J = 8.79 Hz, 2H), 6.03 (s, 2H), 3.86 (t, J = 4.64 Hz, 4H), 3.22 (t, J = 4.88 Hz, 4H), 2.52 (s, 3H), 1.49 (s, 3H) ppm; ^{13}C NMR (125.7 MHz, CD_2Cl_2) δ 155.1, 152.0, 143.6,

142.9, 132.1, 129.1, 125.5, 121.1, 115.6, 66.9, 48.9, 14.6, 14.5 ppm; ^{19}F (282.2 MHz, CD_2Cl_2) δ –146.7 ppm. HRMS (ESI) m/z calcd for $C_{23}H_{26}BF_2N_3O$: 409.2137, found [M-H$^+$]: 410.2220.

Anthracen-9-yl-*N*-(4-nitrophenyl)methanimine (ANI). This compound was synthesized following a modified literature procedure.[S3] 9-Anthraldehyde (0.500 g, 2.4 mmol) and *p*-nitroaniline (0.664 g, 4.8 mmol, 2 equiv) were suspended in absolute ethanol (0.1 M) and refluxed overnight with vigorous stirring. The product precipitates as a dark orange powder, which was filtered and washed with cold ethanol to yield 95 mg of pure **10** in 12% yield. ^{1}H NMR (500 MHz, CD_3CN) δ ^{1}H NMR (500 MHz, CD_3CN) δ 9.77 (s, 1H), 8.90 (dd, *J* = 8.9, 0.8 Hz, 1H), 8.77 (s, 1H), 8.48–8.25 (m, 1H), 8.17 (dd, *J* = 8.4, 0.7 Hz, 1H), 7.71–7.50 (m, 2H) ppm; ^{13}C NMR (125.7 MHz, CD_2Cl_2) δ 162.27, 158.60, 132.45, 131.50, 131.24, 129.46, 128.08, 125.81, 125.30, 124.61, 121.66 ppm. HRMS (ESI) m/z calcd for $C_{21}H_{14}N_2O2$: 326.1055, found [M$^+$]: 326.1063.

Characterization of 1(Zn-*E*). Compound **1(Zn-*E*)** was characterized using ^{1}H NMR spectroscopy (Figure S5), 2D COSY (Figure S6) and 1D NOE (Figure S7) spectroscopies and X-ray crystallography (Figure S34). The spectra were recorded after dissolution of crystals used in the solid state X-ray structure analysis. ^{1}H NMR (500 MHz, CD_3CN): δ 11.95 (s, 1H, Im-NH), 8.94 (dd, *J* = 4.6, 1.4 Hz, 1H, H7), 8.57 (dd, *J* = 8.3, 1.3 Hz, 1H, H5), 8.03 (d, *J* = 7.7 Hz, 1H, H2), 7.78 (dd, *J* = 8.3, 4.6 Hz, 1H, H6), 7.69 (t, *J* = 7.9 Hz, 1H, H3), 7.59 (d, *J* = 8.1 Hz, 1H, H4), 7.36 (t, *J* = 1.6 Hz, 1H, H8), 7.31–7.22 (m, 1H, H9), 4.38 (q, *J* = 7.1 Hz, 2H, -OC*H*$_2$CH$_3$), 1.49 (t, 7.5 Hz, 3H, CH_3) ppm.

3. NMR Spectroscopy

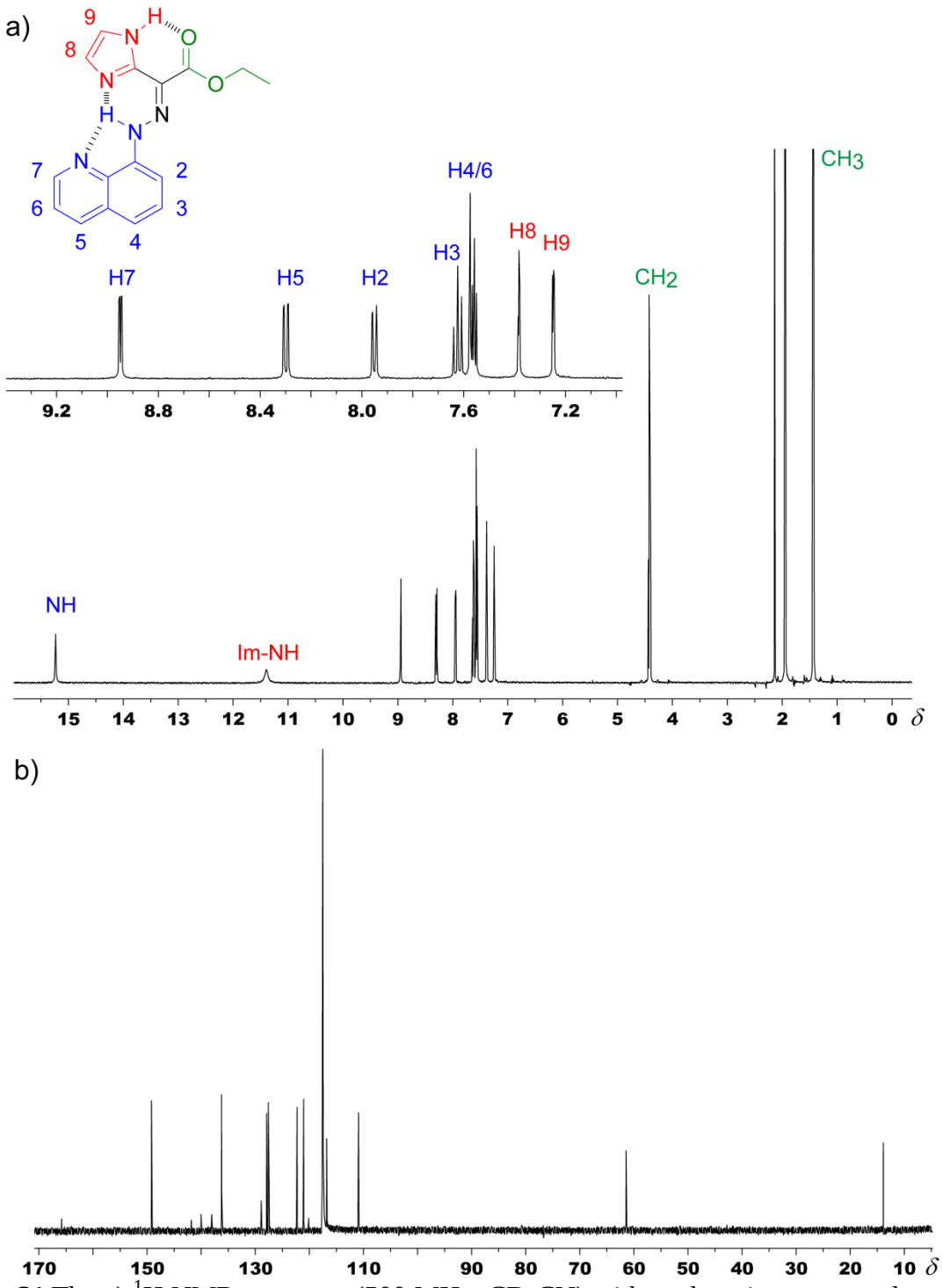

Fig. S1 The a) ^{1}H NMR spectrum (500 MHz, CD_3CN) with peak assignments and a zoom-in on the aromatic region; and b) ^{13}C NMR (125.7 MHz, CD_3CN) spectrum of **1(*E*).**

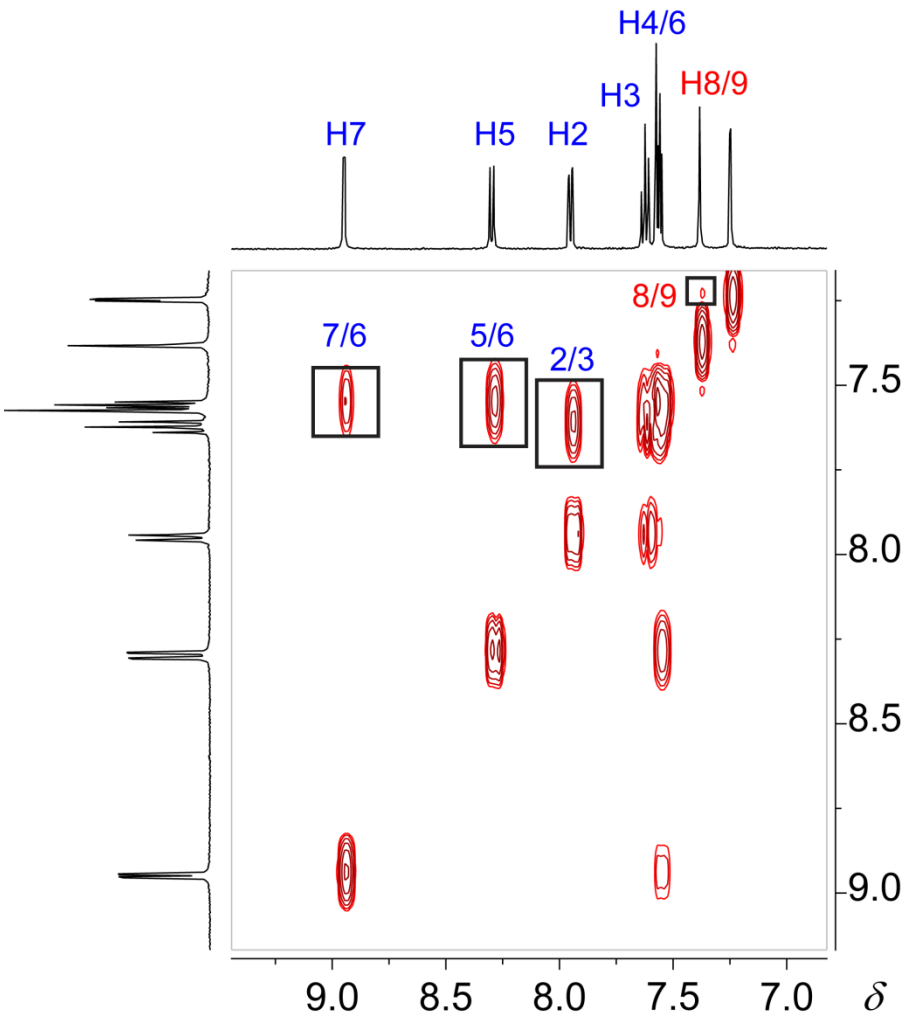

Fig. S2 The 2D COSY spectrum (500 MHz, CD_3CN) of **1(*E*)**.

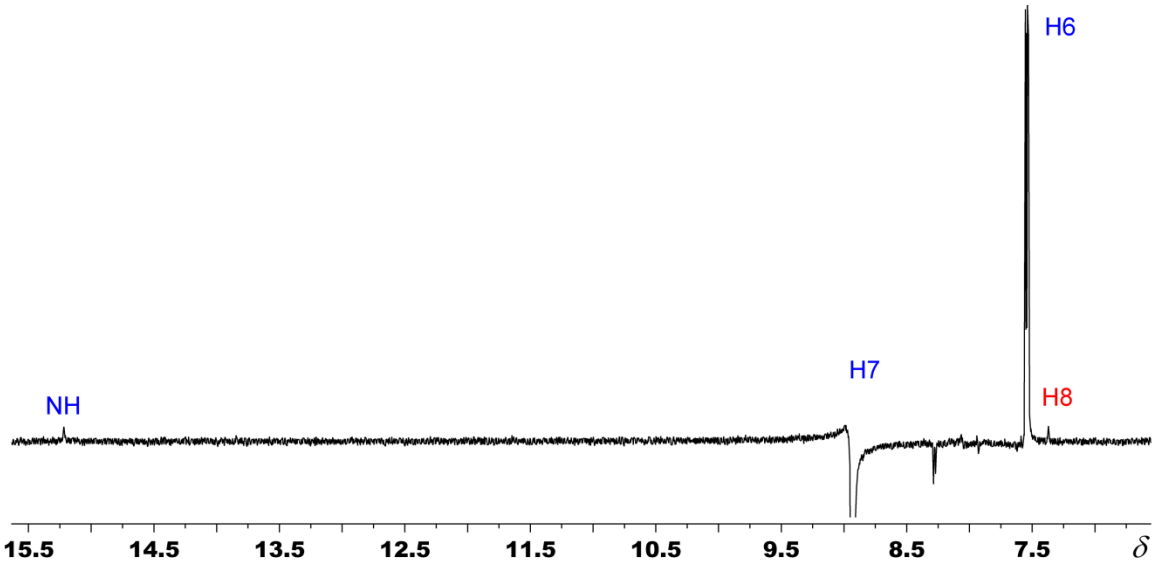

Fig. S3 The 1D NOE spectrum (500 MHz, CD_3CN) of **1(*E*)** showing the correlation between proton H7 and hydrazone NH and H8 protons.

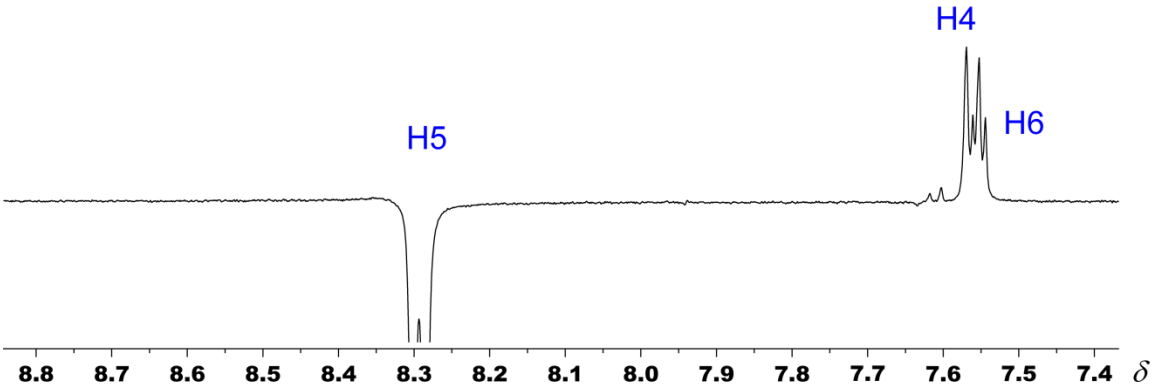

Fig. S4 The 1D NOE spectrum (500 MHz, CD_3CN) of **1(*E*)** showing the correlation between proton H5 and protons H4 and H6.

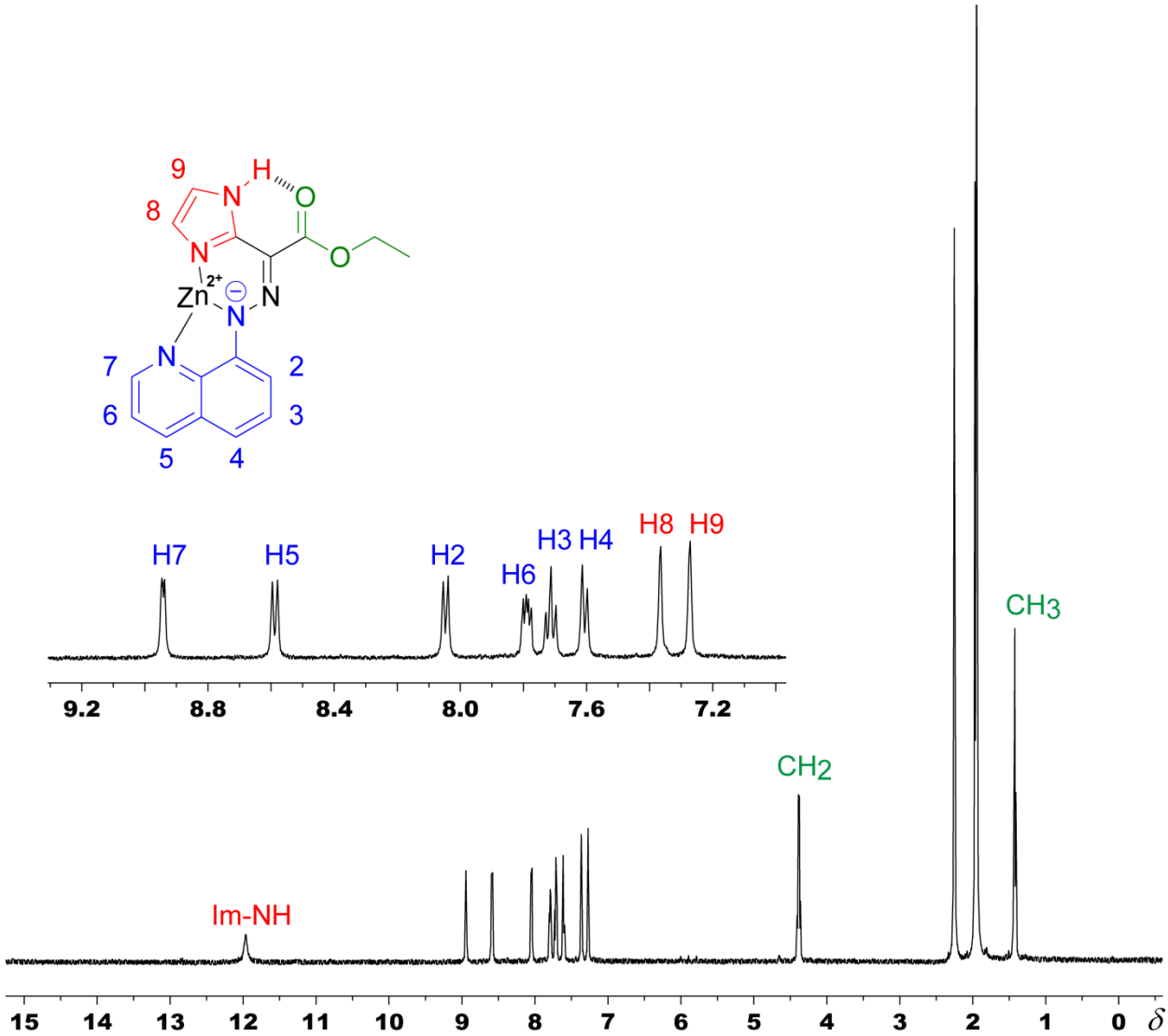

Fig. S5 The ^{1}H NMR spectrum (500 MHz, CD_3CN) of **1(Zn-*E*)** with peak assignments and a zoom-in on the aromatic region.

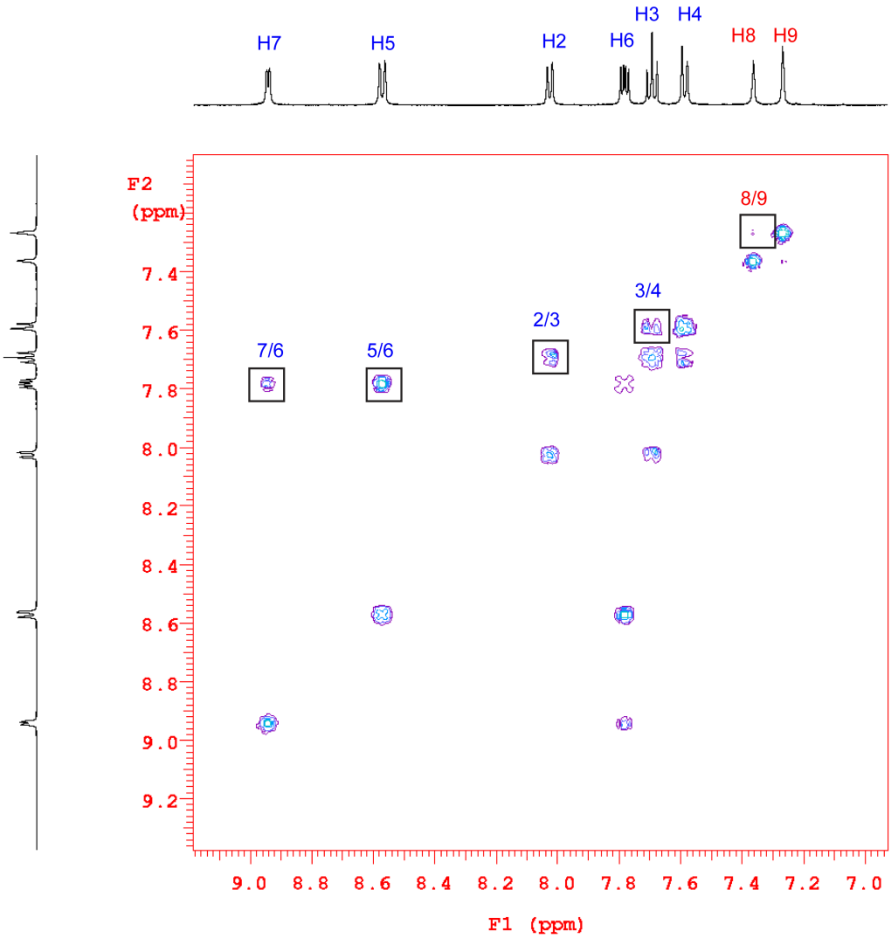

Fig. S6 The 2D COSY spectrum (500 MHz, CD_3CN) of **1(Zn-*E*)**.

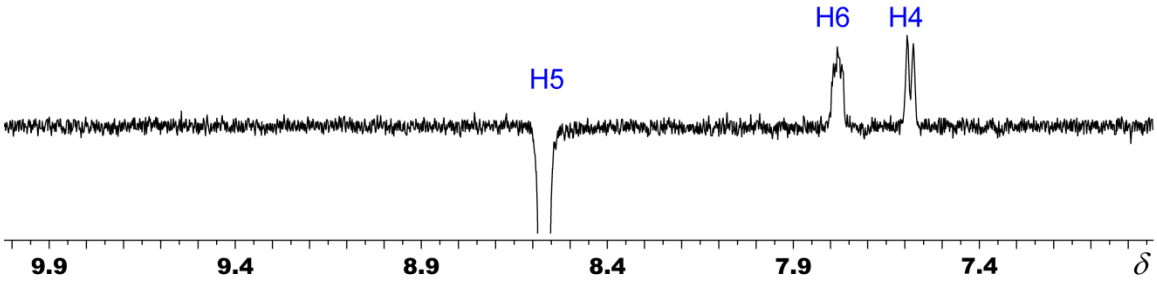

Fig. S7 The 1D NOE spectrum (500 MHz, CD_3CN) of **1(Zn-*E*)** showing the correlation between proton H5 and protons H4 and H6.

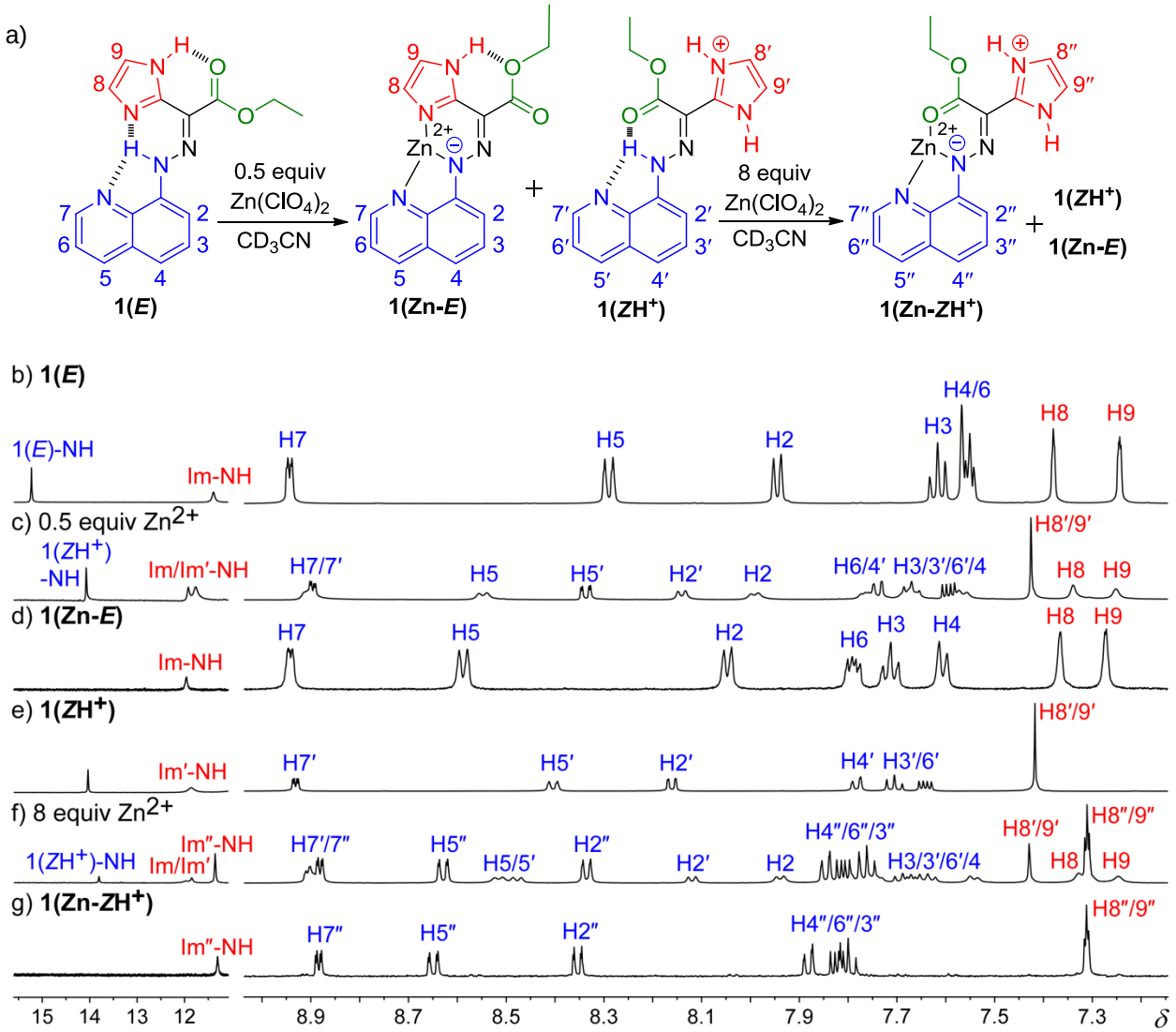

Fig. S8 a) The zinc(II)-initiated CCD scheme with **1(*E*)** demonstrating the different hydrazone species identified using ^{1}H NMR spectroscopy. The ^{1}H NMR spectra (500 MHz, CD_3CN) of b) **1(*E*)**; c) **1(Zn-*E*)** and **1(*ZH*$^{+}$)** obtained after adding 0.5 equiv Zn^{2+} to **1(*E*)**; d) dissolved crystals of **1(Zn-*E*)**; e) **1(*ZH*$^{+}$)** obtained after protonation of **1(*E*)** with TFA (2 equiv); f) the mixture obtained after the addition of 8 equiv Zn^{2+} to **1(*E*)**; and g) **1(Zn-*ZH*$^{+}$)** obtained after adding 1 equiv of Zn^{2+} to **1(*Z*)**.

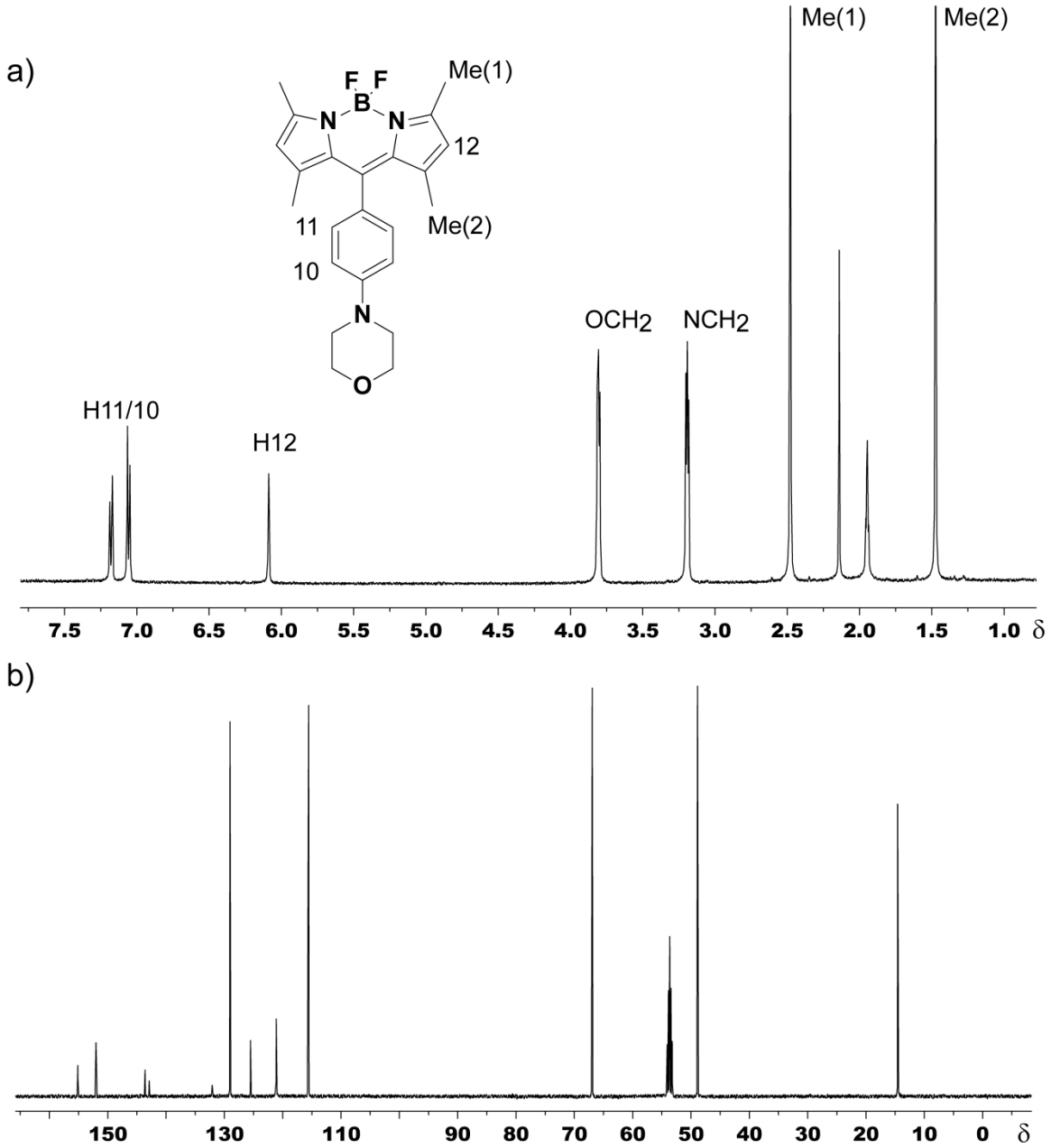

Fig. S9 The a) ^{1}H NMR (500 MHz, CD_3CN), and b) ^{13}C NMR (125.7 MHz, CD_2Cl_2) spectra of **MBD.**

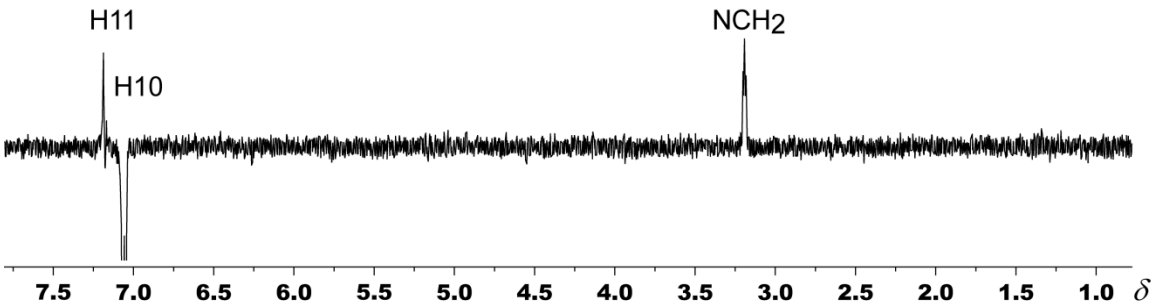

Fig. S10 The 1D NOE spectrum (500 MHz, CD_3CN) of **MBD** showing the correlation between proton H10 and -NCH_2- protons.

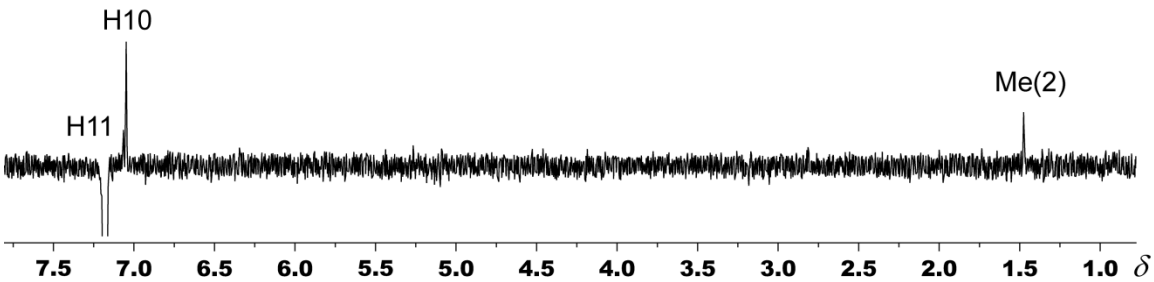

Fig. S11 The 1D NOE spectrum (500 MHz, CD_3CN) of **MBD** showing the correlation between proton H11 and Me(2) protons.

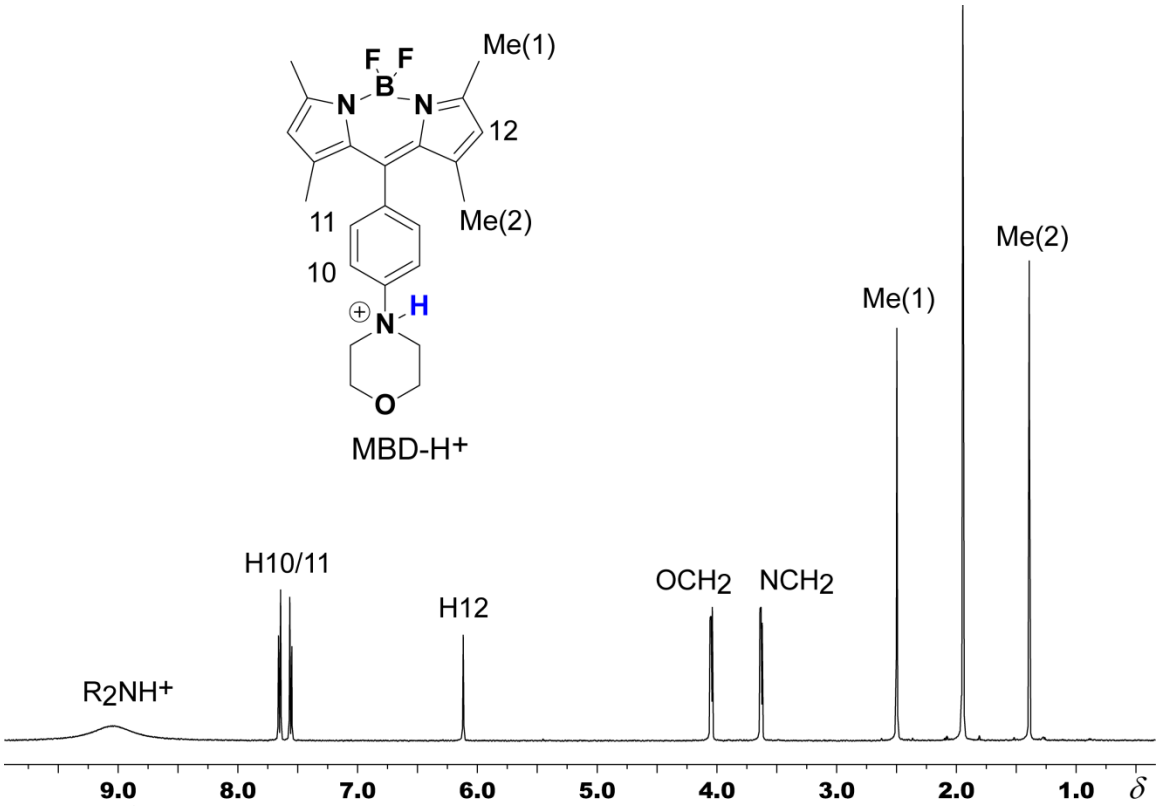

Fig. S12 The ^{1}H NMR spectrum (500 MHz, CD_3CN) of protonated **MBD** (8 equiv TFA).

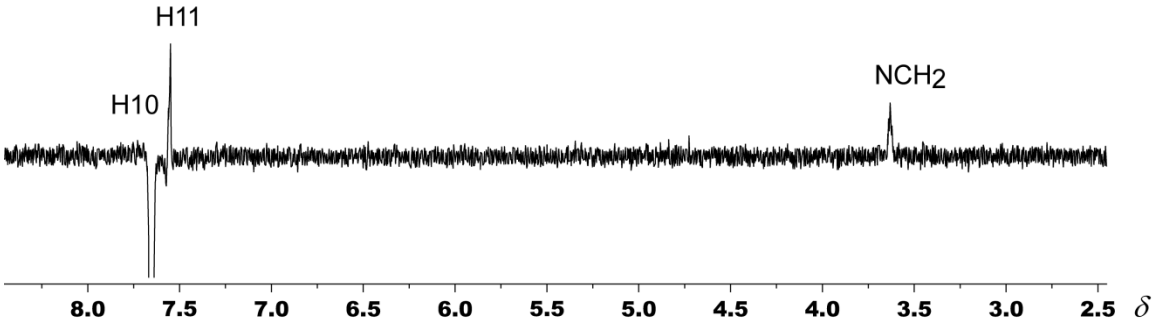

Fig. S13 The 1D NOE spectrum (500 MHz, CD_3CN) of **MBD-H$^+$** showing the correlation between proton H10, and H11 and -NCH_2- protons.

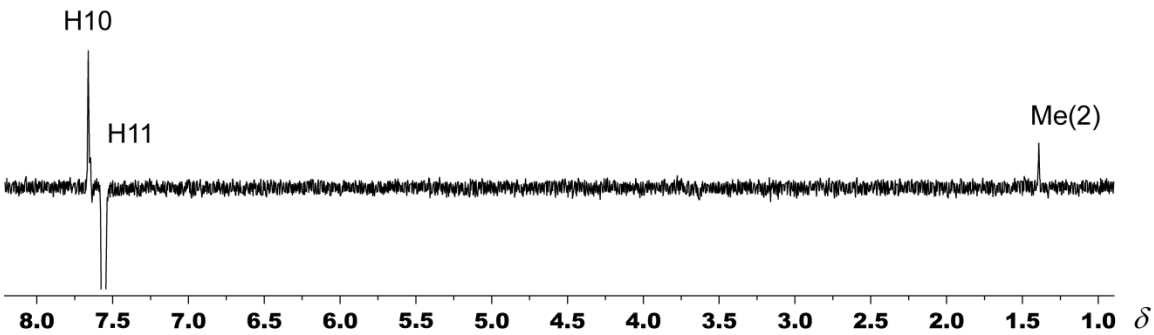

Fig. S14 The 1D NOE (500 MHz, CD_3CN) of **MBD-H**$^+$ showing the correlation between proton H11 and proton H10 and Me(2) protons.

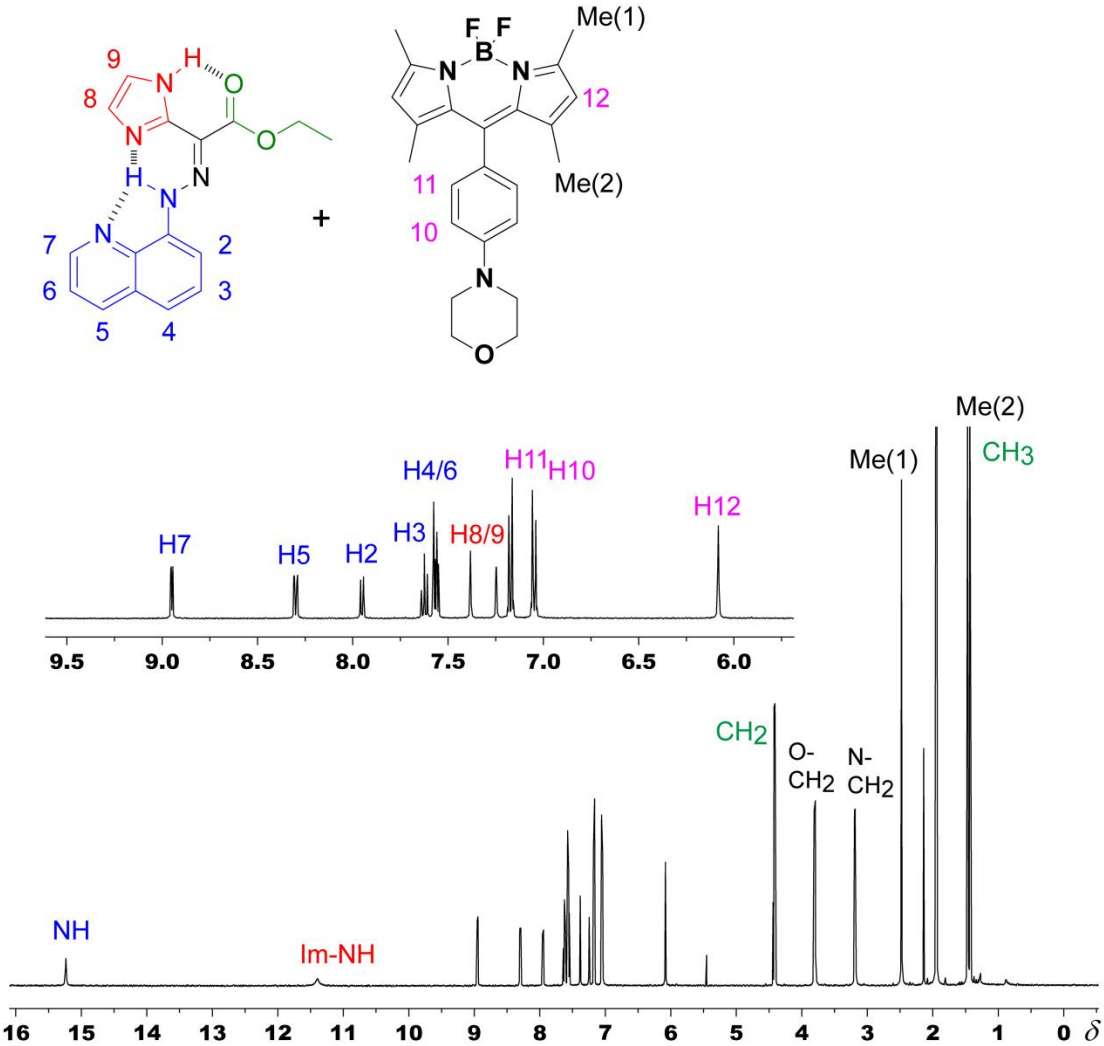

Fig. S15 The ^{1}H NMR spectrum (500 MHz, CD_3CN) of a 1:1 mixture of **1(*E*)** and **MBD**, including a zoom-in on the aromatic region.

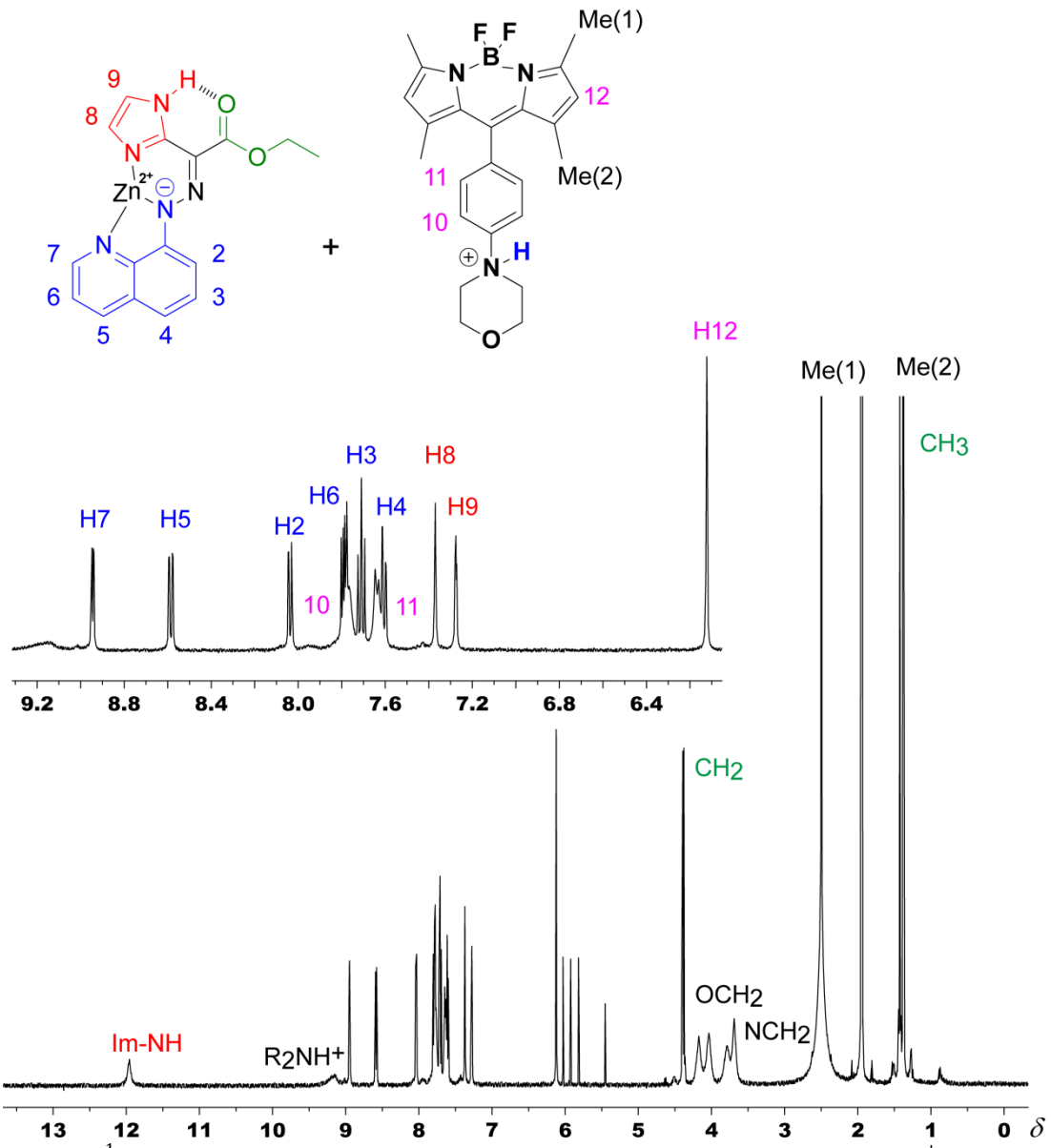

Fig. S16 The ^{1}H NMR spectrum (500 MHz, CD_3CN) of **1(Zn-*E*)** and **MBD-H$^+$** obtained after the addition of $Zn(ClO_4)_2$ (1 equiv), including a zoom-in on the aromatic region.

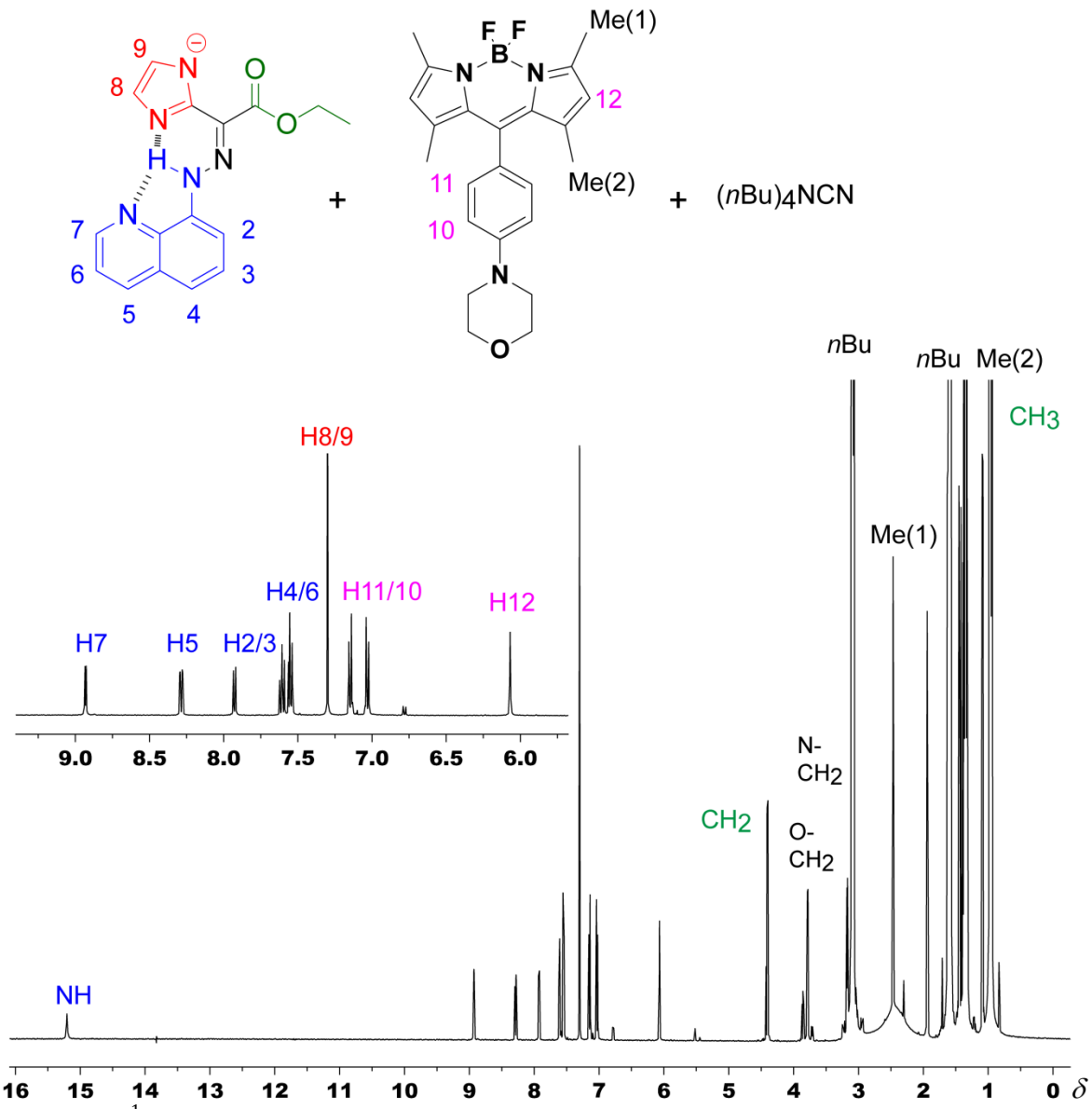

Fig. S17 The ^{1}H NMR spectrum (500 MHz, CD_3CN) of **1(*E*)** and **MBD** after addition of excess (nBu)$_4$NCN (7 equiv) to **1(Zn-*E*)** and **MBD-H$^+$**, including a zoom-in on the aromatic region. The addition of excess CN^- causes the deprotonation of the imidazolyl-NH proton.

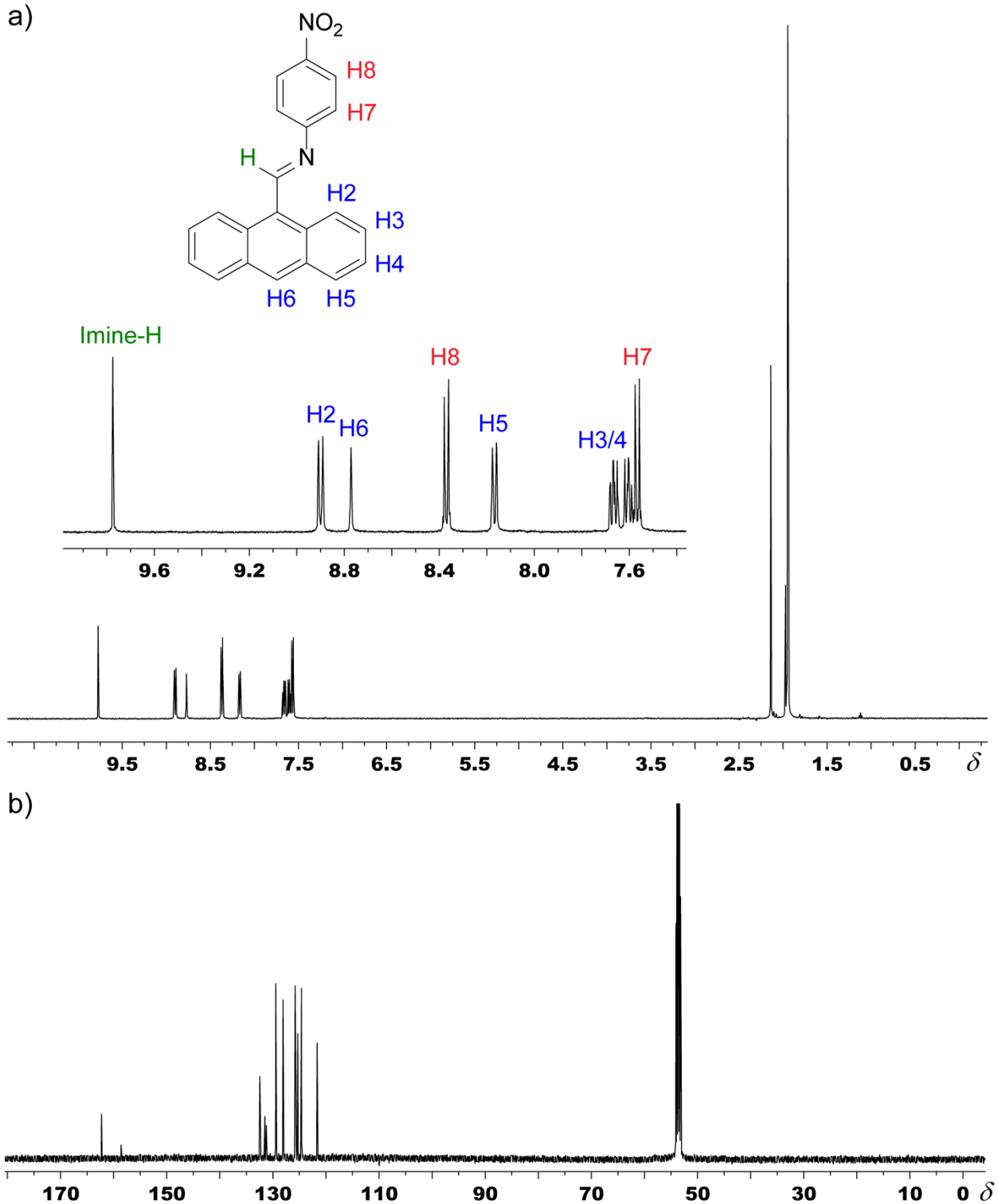

Fig. S18 The a) ^{1}H NMR spectrum (500 MHz, CD_3CN) with a zoom-in on the aromatic region, and b) ^{13}C NMR spectrum (125.7 MHz, CD_2Cl_2) of **ANI**.

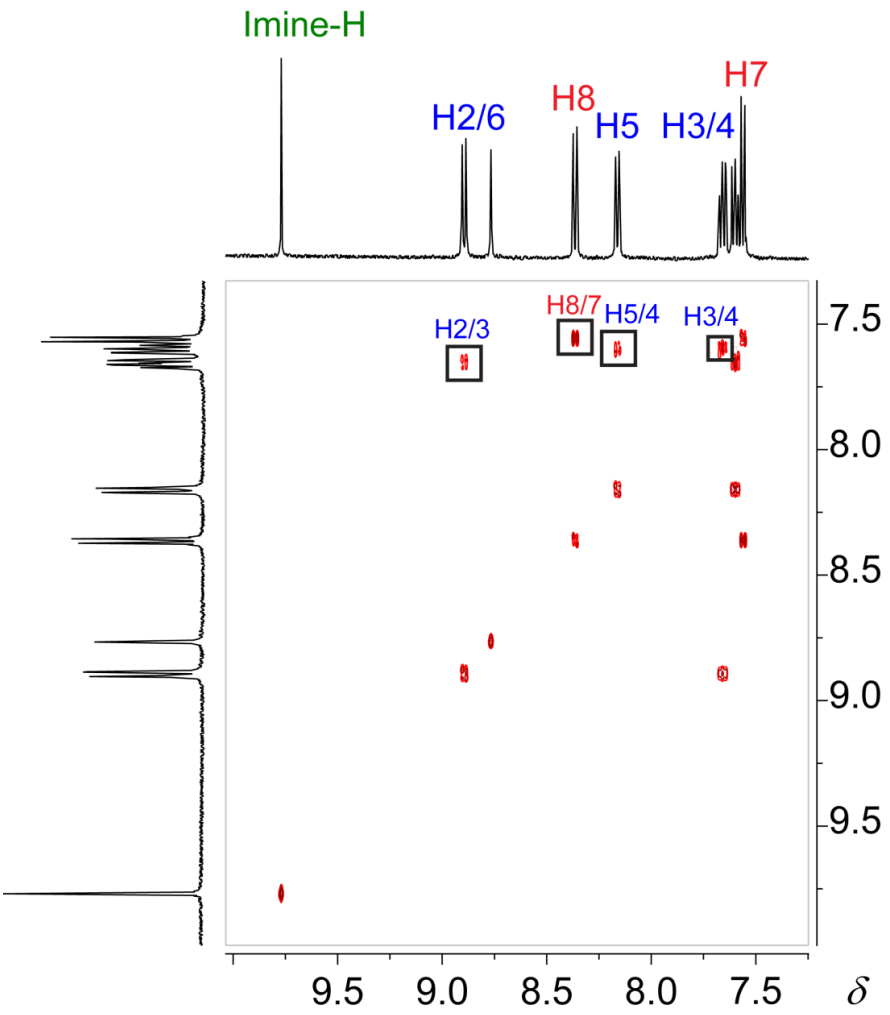

Fig. S19 The 2D COSY spectrum (500 MHz, CD_3CN) of **ANI**.

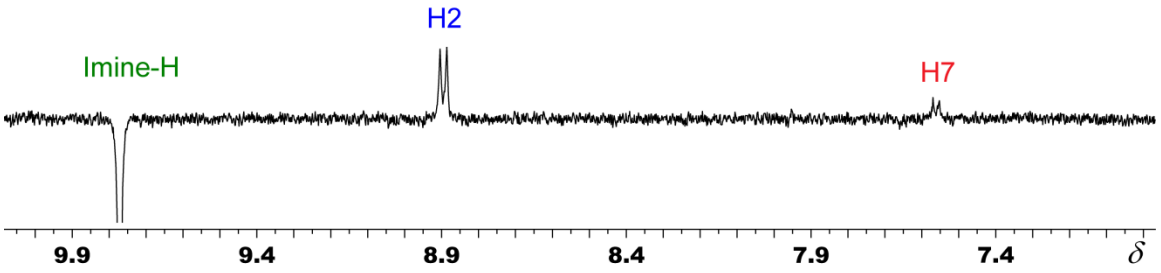

Fig. S20 The 1D NOE spectrum (500 MHz, CD_3CN) of **ANI** after irraditation of the imine proton showing the correlation between protons H2 and H7.

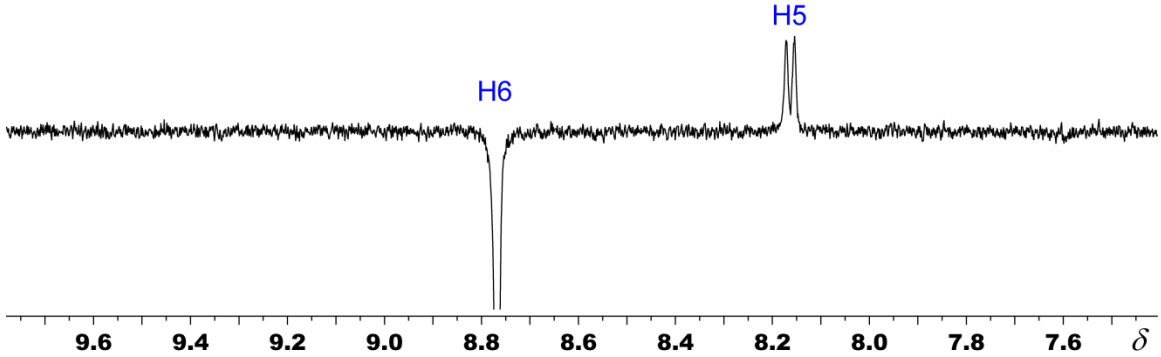

Fig. S21 The 1D NOE spectrum (500 MHz, CD_3CN) of **ANI** after irradiation of proton H6 showing the correlation between proton H5.

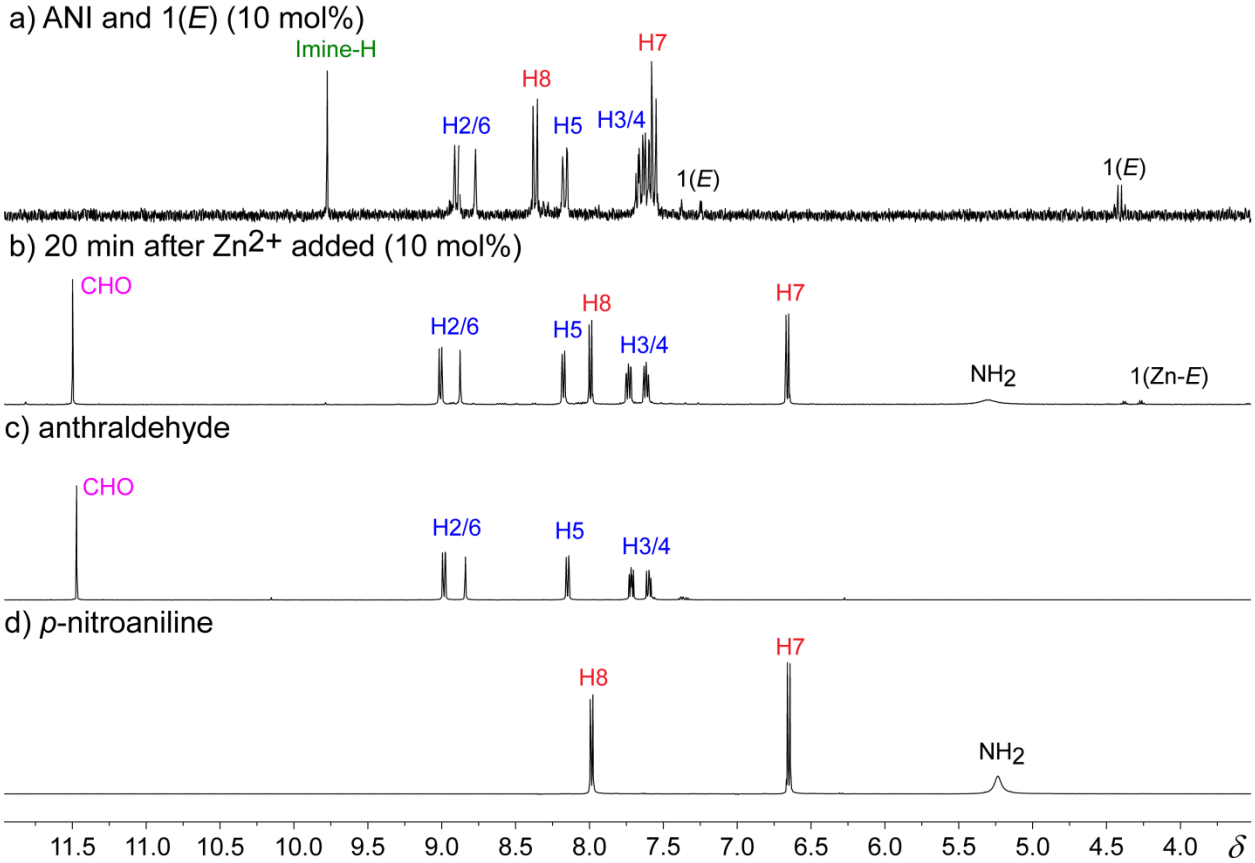

Fig. S22 The ^1H NMR spectra (500 MHz, CD_3CN) of a) **ANI** and **1(*E*)** (10 mol%); b) the mixture 30 min after the addition of 10 mol% Zn^{2+}, demonstrating complete hydrolysis of the imine (> 99%); c) anthraldehyde, and d) *p*-nitroaniline.

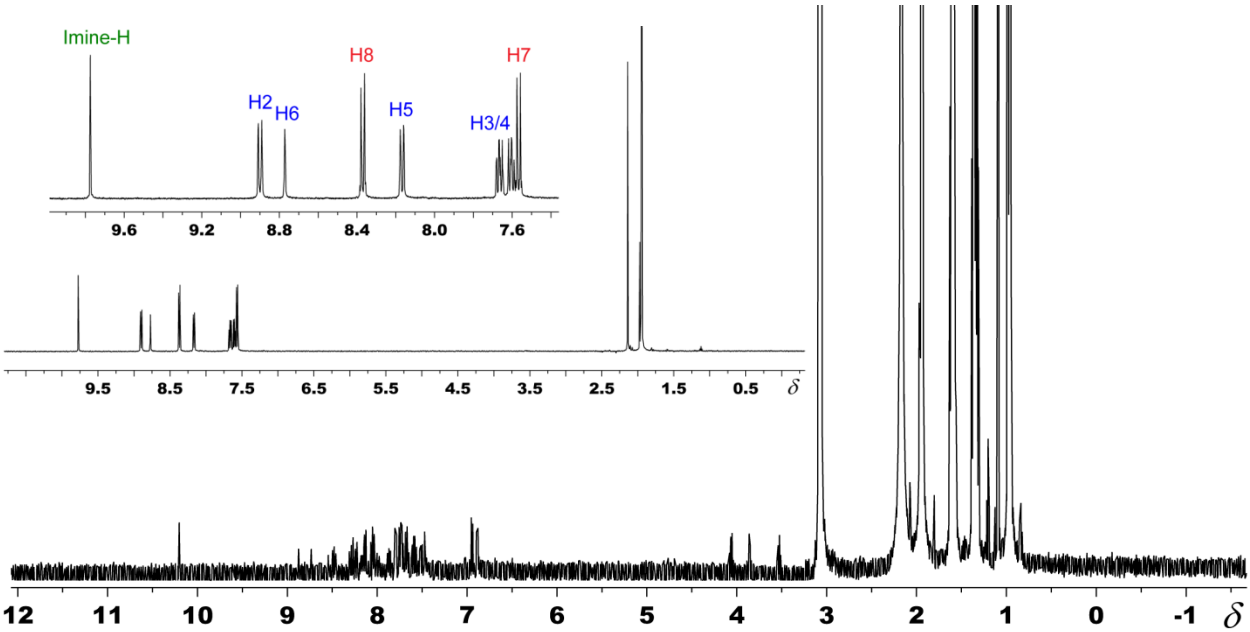

Fig. S23 The ^{1}H NMR spectrum (500 MHz, CD_3CN) of **ANI** with 1 equiv of CN^-. A comparison with the spectrum of **ANI** (inset and Figure S18) shows that a reaction occurred between the two. The product of the reaction has low solubility and hence the weak signals.

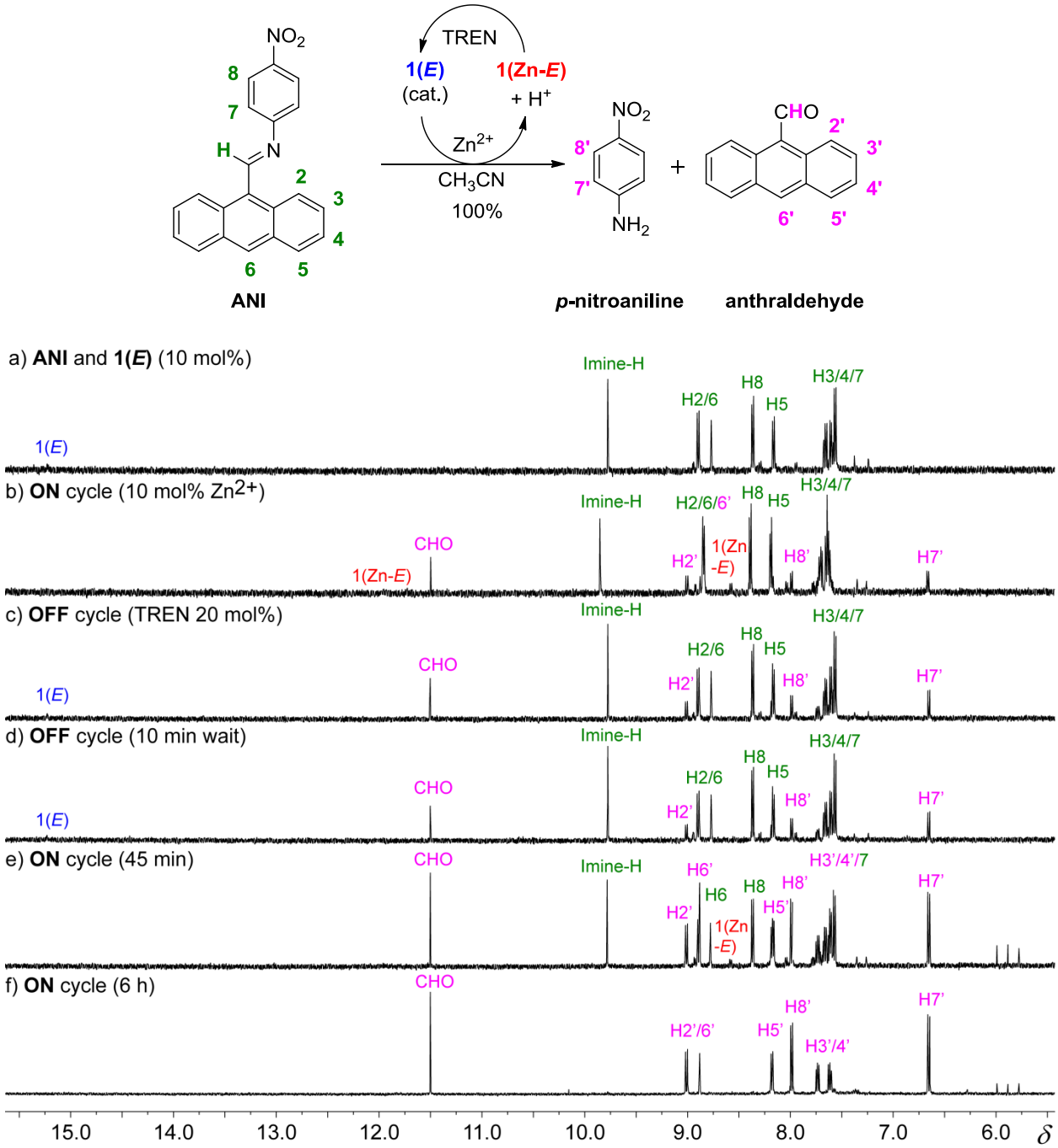

Fig. S24 The ^{1}H NMR spectra (500 MHz, CD_3CN) of a) **ANI** and **1(*E*)** (10 mol%); b) hydrolysis of **ANI** and formation of anthraldehyde obtained after addition of $Zn(ClO_4)_2$ (10 mol%) and formation of **1(Zn-*E*)** (6 min); c) addition of TREN (20 mol%) shuts "off" the hydrolysis by restoring **1(*E*)**; d) the resulting spectrum after 10 min demonstrating no additional hydrolysis of **ANI**; e) addition of $Zn(ClO_4)_2$ (40 mol%) turns catalysis back "on" with the formation of **1(Zn-*E*)** (45 min); and g) the complete hydrolysis of **ANI** observed after 6 h.

4. Absorption and Fluorescence Spectra

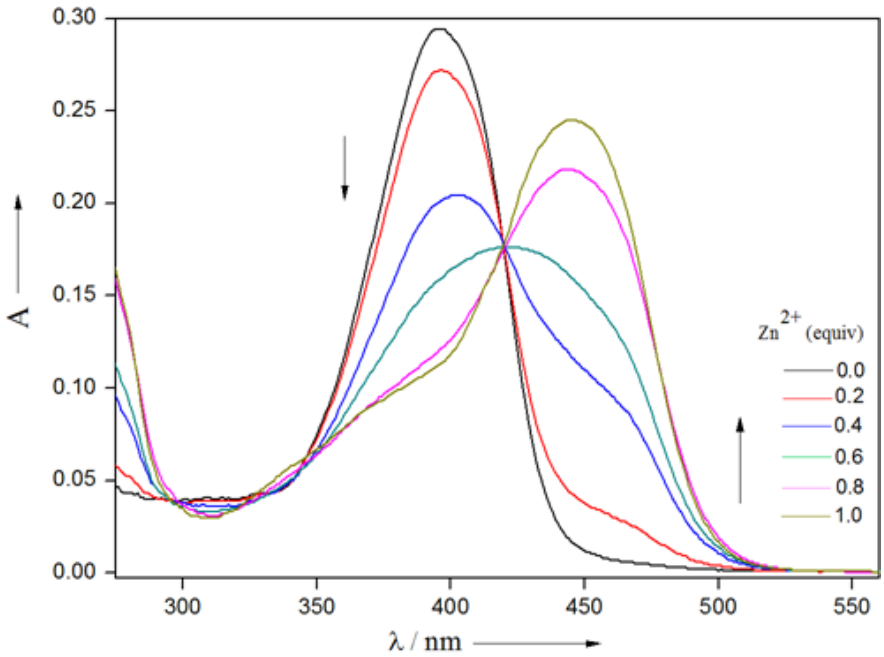

Fig. S25. The UV/Vis spectra of the titration of **1(*E*)** (1×10^{-5} M, CH_3CN) with increasing amounts of Zn^{2+} ions, in the presence of 1 equiv of base (Et_3N), which acts as a proton sponge.

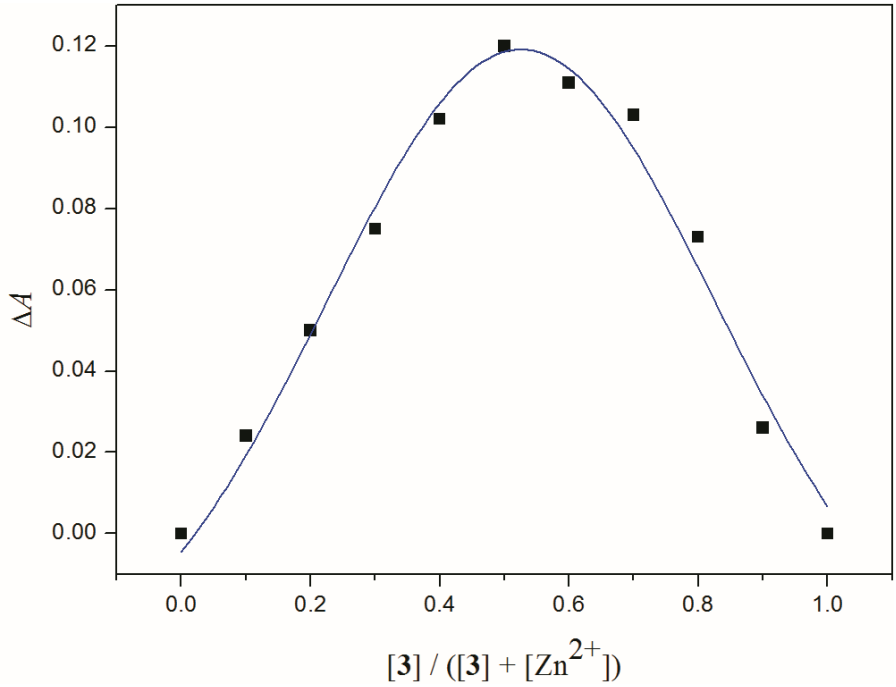

Fig. S26. The Job's plot obtained from the titration experiment with **1(*E*)**.

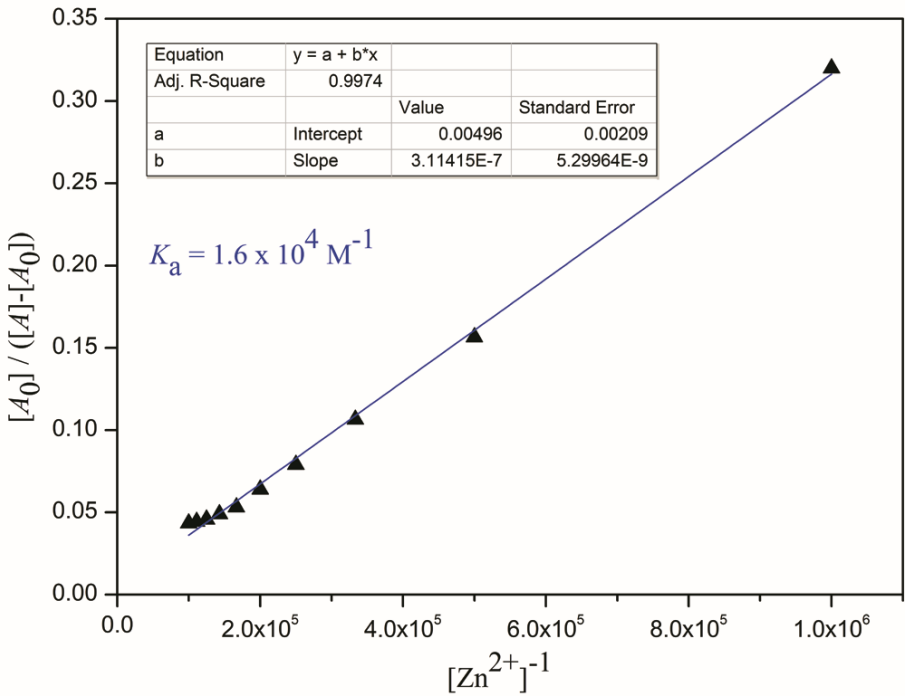

Fig. S27. The binding constant calculation plot between **1(*E*)** and zinc(II). The titration was done in the presence of 1 equiv of base (Et_3N), which acts as a proton sponge.

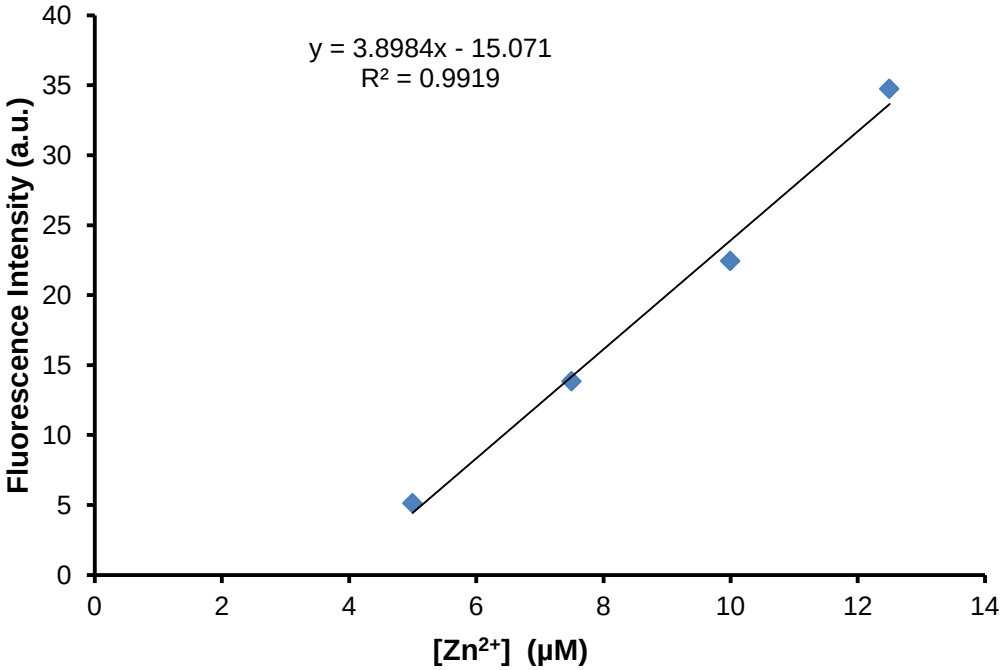

Fig. S28. The LOD plot of **1(*E*)** and **MBD** (1:1 mixture, 5×10^{-5} M, CH_3CN) monitoring the fluorescence with increasing amounts of zinc(II).

5. Control Studies

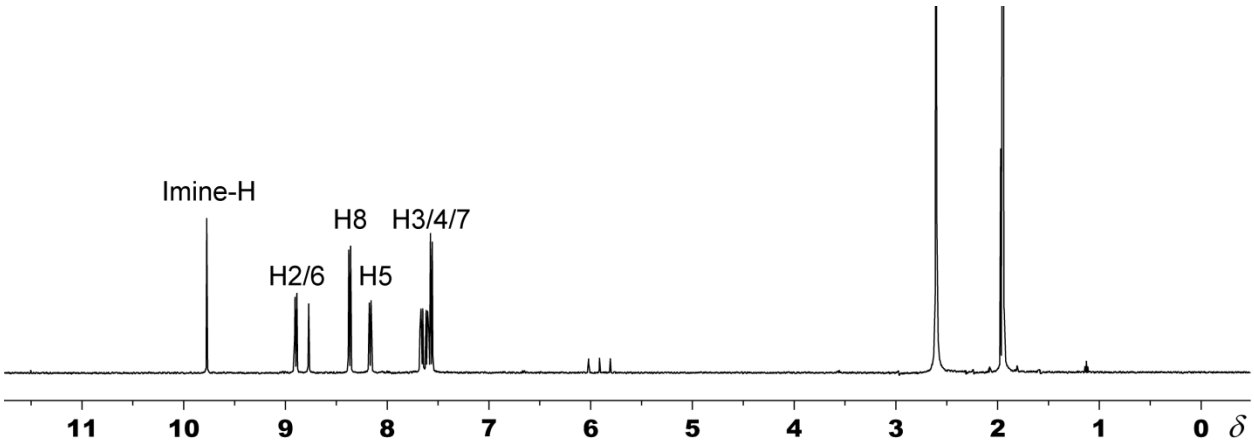

Fig. S29 The ^{1}H NMR spectrum (500 MHz, CD_3CN) of **ANI** with 1 equiv $Zn(ClO_4)_2$, showing no changes in the signals even after 1 h.

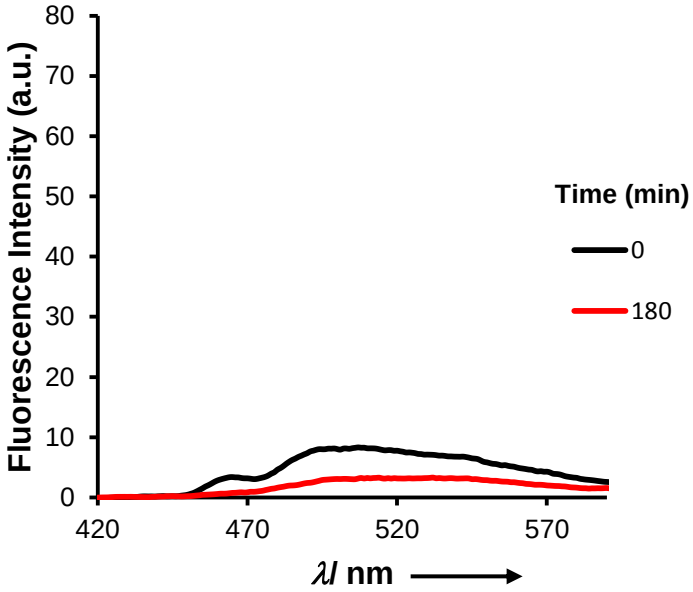

Fig. S30 The fluorescence spectra (5×10^{-5} M, CH_3CN) of **ANI** after the addition of $Zn(ClO_4)_2$ (10 mol%).

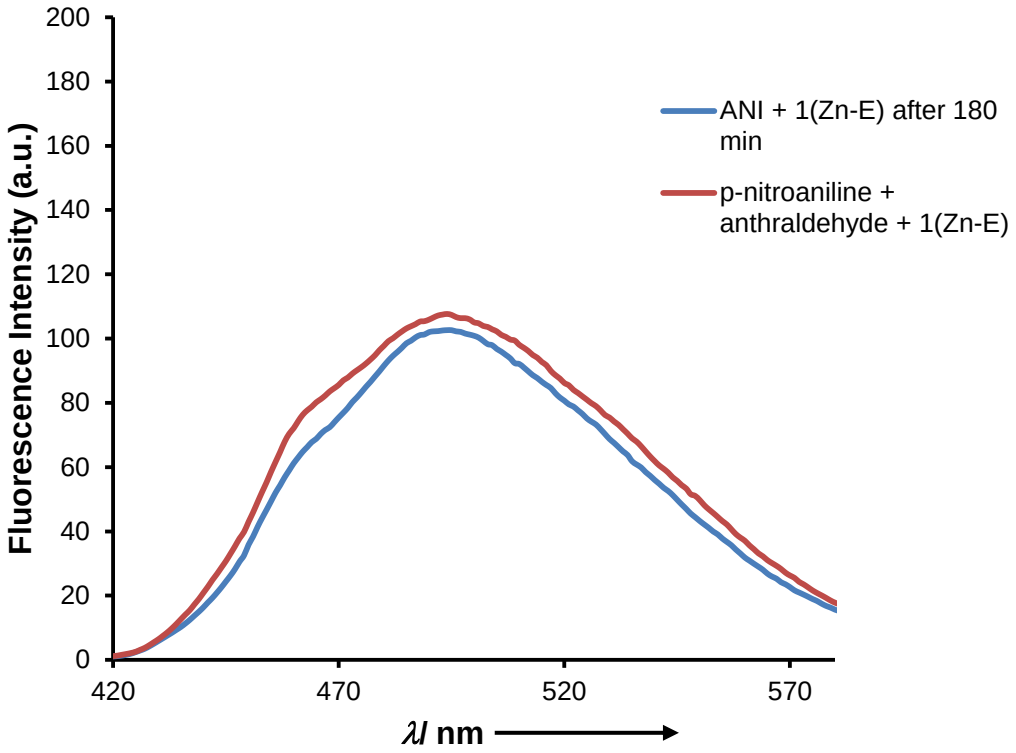

Fig. S31 The control experiment demonstrating that the hydrolysis of **ANI** went to near completion after 180 min (blue line) compared to the control of *p*-nitroaniline, anthraldehyde (1:1 mixture, 5×10^{-5} M) in the presence of **1(Zn-*E*)** (10 mol%) (red line).

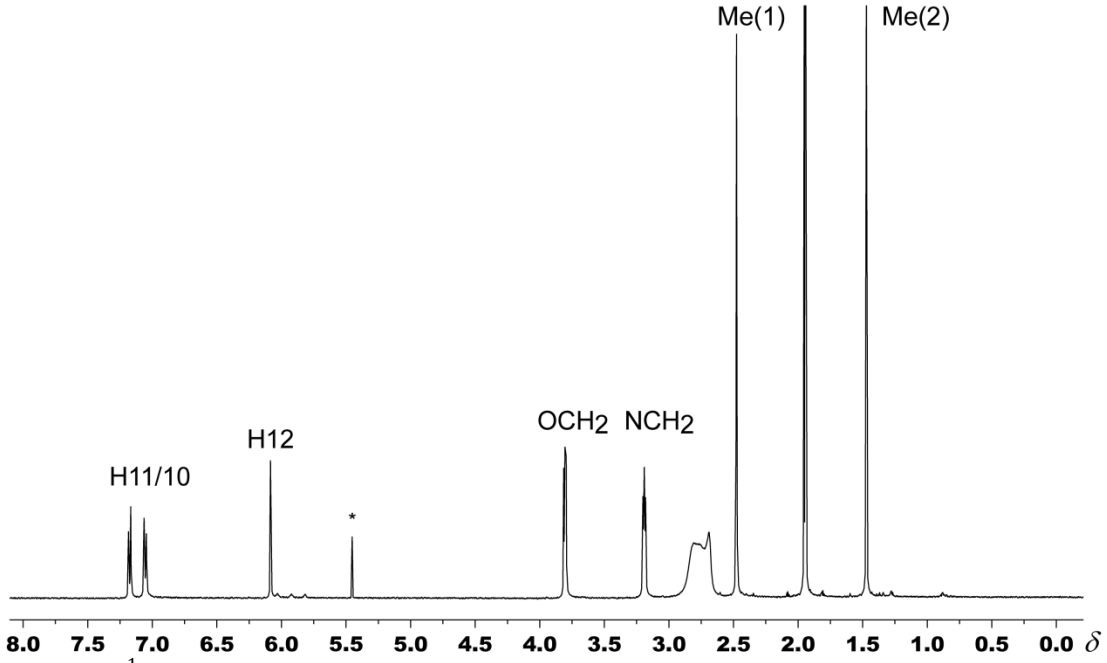

Fig. S32 The ^{1}H NMR spectrum (500 MHz, CD_3CN) of **MBD** and $Zn(ClO_4)_2$ (2 equiv). * denotes residual dichloromethane on the sample.

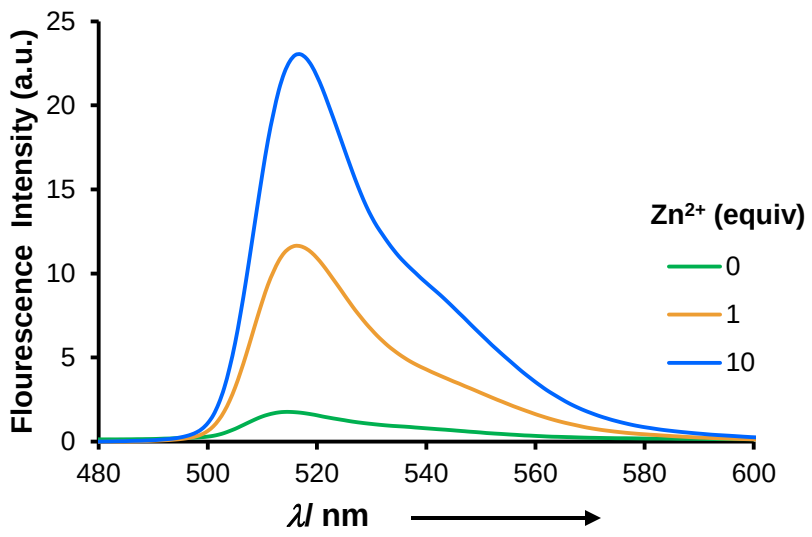

Fig. S33 The fluorescence spectra (5×10^{-5} M, CH_3CN) of **MBD** with increasing amounts of $Zn(ClO_4)_2$, showing a minimal increase in emission.

6. X-Ray Crystal Data

Data were collected using a Bruker CCD (charge coupled device) based diffractometer equipped with an Oxford Cryostream low-temperature apparatus operating at 173 K. Data were measured using ω and ξ scans of 0.5° per frame for 30 s. The total number of images was based on results from the program COSMO[S4] where redundancy was expected to be 4.0 and completeness of 100% out to 0.83 Å. Cell parameters were retrieved using APEX II software[S5] and refined using SAINT on all observed reflections. Data reduction was performed using the SAINT software[S6] which corrects for Lp. Scaling and absorption corrections were applied using SADABS[S7] multi-scan technique, supplied by George Sheldrick. The structures are solved by the direct method using the SHELXS-97 program and refined by least squares method on F^2, SHELXL- 97, which are incorporated in SHELXTL-PC V 6.10.[S8] All non-hydrogen atoms are refined anisotropically. Hydrogens were calculated by geometrical methods and refined as a riding model except for those on the nitrogen atoms N1, N4 and N5 and of the water molecule. These hydrogens were found by difference Fourier methods and refined.

7. References

S1 D. Ray, J. T. Foy, R. P. Hughes and I. Aprahamian, *Nature Chem.*, 2012, **4**, 757–762.

S2 S. Hoogendorn, A. E. M. Blom, L. I. Willems, G. A. v. d Marel, H. S. Overkleeft, *Org. Lett.*, 2012, **13**, 5656–5659.

S3 N. Giuseppone, J.-L. Schmitt, E. Schwartz, J.-M. Lehn, *J. Am. Chem. Soc.*, 2005, **127**, 5528–5539.

S4 COSMO V1.58 software for the CCD detector systems for determining data collection parameters. Bruker analytical X-ray systems (Madison, WI, USA 2008).

S5 APEX2 V2008.5-0 software for the CCD detector system. Bruker analytical X-ray systems (Madison, WI, USA 2008).

S6 SAINT V 7.34 software for the integration of CCD detector system. Bruker analytical X-ray systems (Madison, WI, USA 2008).

S7 R. H. Blessing, "An empirical correction for absorption anisotropy", *Acta. Cryst. A, 1995*, **51**, 33–38.

S8 G. M. Sheldrick, "A short history of SHELX",. *Acta. Cryst. A*, 2008, **64**, 112–122.